Polymer Bulletin 14, 61–68 (1985)

Polymer Bulletin

Deformation

Macroscopic and Crystallographic Density of Solid-State Extruded Polyethylene

Raúl E. De Micheli[1], Haydee M. Vidal[2], and Edgardo M. Macchi[3]

[1] Centro de Investigaciones Tecnológicas para la Industria Plástica-INTI, Casilla de Correo 157, 1650 San Martín, Argentina

[2] Departamento de Química-INTI, Casilla de Correo 157, 1650 San Martín, Argentina

[3] Division Macromoléculas-INIFTA, Cassila de Correo 16, Suc. 4, 1900 La Plata, Argentina

SUMMARY

The influence of draw ratio on macroscopic and crystallographic density of polyethylene with different initial morphologies, has been investigated by solid-state extrusion. An initial drop followed by an increase in macroscopic density as a function of draw ratio has been observed. Since precision X-ray measurements of unit cell parameters showed no variation of crystallographic density, it was concluded that plastic deformation of polyethylene upon drawing proceeds with a decrease of the degree of crystallinity. This was confirmed by differential scanning calorimetry.

INTRODUCTION

Deformation of semicrystalline polymers by cold drawing or by solid-state in hydrostatic extrusion proceeds with well-defined changes on the observed macroscopic density (D_m), consisting on an initial drop and a subsequent increase as a function of nominal draw ratio (NDR). The corresponding density minima, centered at NDR between 2 and 7 have been observed by several authors (1,2) particularly in the case of deformation processes carried out at temperatures well below the crystalline melting points of the corresponding polymers.

This remarkable behavior obviously results from the combined play of two independent and opposite effects contributing with a monotonic decrease and a monotonic increase in density respectively over the whole range of studied NDR (3). From the point of view of the two-phase model, effects related to molecular orientation in amorphous regions, especially an increase in the fraction of unidirectionally oriented, but still amorphous tie molecules, provide a morphological basis for the interpretation of the effects responsible for the monotonic increase in density. This last phenomenon has been studied by Glenz et al. (3), who claim an increase in noncrystalline density during drawing of about 5% for the highest possible NDR 25. After Glenz et al., then, the effect which brings about the density increase is clearly related to only one of the two phases of the model, i.e. the amorphous one.

What is, then, the molecular mechanism responsible for the density decrease. Two simple hypotheses can be formulated. First, a variation in unit cell dimensions would result in a corresponding variation of the polymer crystallographic density or, secondly, a decrease in the total fraction of crys-

talline material. The goal of the present investigation, therefore, is to elucidate the mechanism responsible for the monotonic decrease in density. To this end, a systematic study on the deformation of high density polyethylene (HDPE) will be performed, whereby, not only NDR but also initial morphology of the specimens and deformation temperatures will be varied over carefully defined ranges. Deformation processes will be carried out by solid-state extrusion (SSE) in order to avoid the formation of interfibrillar voids, a third phase not taken into account in the previous discussion based on the two-phase model. Finally, the characterization of the specimens, original as well deformed, will be approached by measurements of macroscopic density and heat of fusion, and by precision determination of lattice parameters.

EXPERIMENTAL

Void-free HDPE pellets (Alathon 7050, $\bar{M}w$ = 59,000 $\bar{M}n$ = 19,000) were melted and crystallized at a series of temperatures and pressures as described elsewhere (2). In this way, billets of different morphologies ranging from folded-chain (FCC) to extended-chain (ECC) crystals were obtained. SSE of the preformed billets was carried out through a conical die with 20° entrance angle, according to a technique developed and extensively employed by Porter et.al. (4). Densities of extruded and original undeformed samples were measured at 23°C, in a gradient column to an accuracy of 1.5 x 10^{-3} g/cm^3, using a mixture of ethanol and 1% glycerol solution in water (ASTM D-1505). Independently, degree of crystallinity data were obtained by quantitative differential scanning calorimetry by means of a Perkin-Elmer DSC-2 instrument (scanning rate 10°C per minute, heat of fusion of PE crystal 69 cal/g).

Precision lattice parameter measurements were carried out in a highly reproducible way by either diffractometric or photographic methods with silicon external or α-quartz powder internal calibration standards respectively, depending upon the nature of the specimens. To reach the highest possible accuracy, the measurements were carried out observing the following precautions: 1.-All low-order reflections, which display the largest errors (5), were excluded from the analysis. 2.- To still increase the values of the Bragg angles, the extruded specimens were measured not with the usual Cu Kα radiation (λ = 1.5405 Å), but with Co Kα radiation (λ = 1.7889 Å) 3.- Accurate lattice parameters and the corresponding standard deviations were calculated by means of a least squares procedure (6) over a relatively large number of independent reflections. Since even in the most favorable cases, however, the highest reachable Bragg angle was 37.25° (Cu radiation and 5 2 0 reflection), no mathematical procedure for extrapolation to Θ = 90° (7) could possibly be undertaken.

Isotropic, undeformed samples were investigated by means of a Philips PW 1050/25 vertical goniometer with a step scan unit, programmer and proportional detector. The solid-state extruded specimens were analysed using a Weissenberg cammera with Fe-filtered Co Kα radiation. Two different geometrical set ups were employed to register the equatorial and meridional reflections,respectively. The positions of the reflections were read visually with the help of a precision comparator.

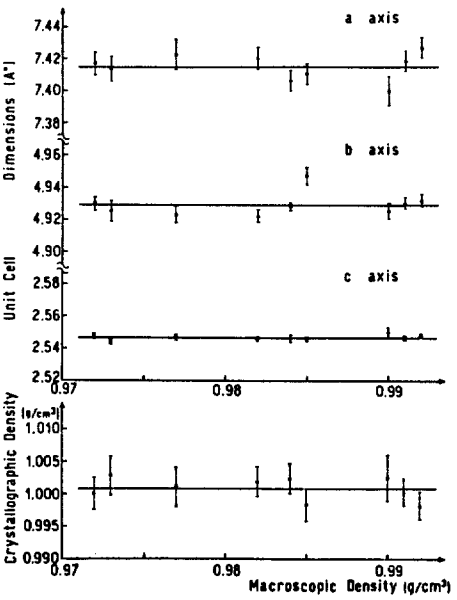

Fig. 1 Unit cell dimensions and corresponding crystallographic densities as a function of macroscopic density of undeformed PE samples prepared at different pressures and temperatures.

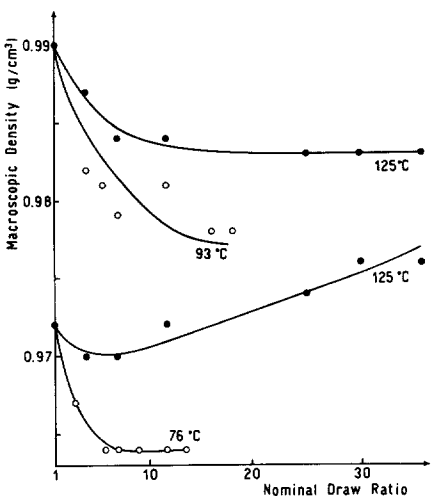

Fig. 2 Macroscopic density vs. nominal draw ratio for SSE samples with two different initial morphologies, prepared at two different temperatures each.
- ● ECC at 125°C
- o ECC at 93°C
- ● FCC at 125°C
- o FCC at 76°C

RESULTS AND DISCUSSION

As a starting material for the SSE, a series of samples ranging from folded-chain (Dm = 0.972 g/cm^3) to extended-chain (Dm = 0.992 g/cm^3) morphology were prepared by crystallization at different temperatures and pressures (8). Table I shows the macroscopic densities of the specimens thus obtained, together with the corresponding crystal data, calculated crystallographic densities and percent crystallinity. The plot in Fig. 1 clearly shows that, within the limits of the experimental errors, there is no variation of crystallographic density over the whole range of studied morphologies. SSE of these samples was carried out at temperatures ranging from 76°C to 125°C, and NDR from 1 to 36. Low temperature extrusion, 76°C and 93°C, was limited to maximum NDR 13.5 and 18, respectively, due to the extremely high pressures involved, whereby, NDR 11.7 and 16 already marked the onset of fracture processes. Fig. 2 displays the dependence of macroscopic density on nominal draw ratio for samples with two different initial morphologies, corresponding to FCC, Dm = 0.972 g/cm^3, percent crystallinity = 77, and ECC, Dm = 0.990 g/cm^3, percent crystal-

D_m* (g/cm^3)	Percent Crystallinity	D_x (g/cm^3)	a axis (A°)	b axis (A°)	c axis (A°)	Number of measured reflections
0.992	97	0.998±0.002	7.426±0.007	4.932±0.004	2.548±0.001	15
0.991	95	1.000±0.002	7.418±0.006	4.930±0.004	2.546±0.001	15
0.990	92	1.002±0.004	7.400±0.009	4.925±0.005	2.550±0.003	11
0.985	90	0.998±0.003	7.410±0.006	4.947±0.005	2.545±0.001	15
0.984	89	1.002±0.002	7.406±0.007	4.928±0.003	2.546±0.002	12
0.982	87	1.002±0.002	7.420±0.007	4.922±0.004	2.546±0.001	16
0.977	82	1.001±0.003	7.422±0.009	4.923±0.005	2.547±0.002	16
0.973	78	1.003±0.003	7.413±0.008	4.925±0.007	2.544±0.002	14
0.972	77	1.000±0.003	7.417±0.007	4.930±0.004	2.547±0.002	15

Table I. Macroscopic (D_m) and crystallographic (D_x) density, and percent crystallinity from DSC data for isotropic samples crystallized at different pressures and temperatures. Number of reflections used for unit cell parameters calculations is denoted for each sample.

(*) Precision: ±0.0015 g/cm^3.

ORIGINAL MORPHOLOGY	EXTRUSION CONDITIONS		E X T R U D A T E S					
D_m^* (g/cm^3)	NDR Temperature (°C)		D_m^* (g/cm^3)	Percent Crystallinity	D_x (g/cm^3)	a axis (A°)	b axis (A°)	Number of measured lines
0.990	11.7	125	0.984	89	0.997±0.002	7.426±0.006	4.942±0.002	6
0.990	36.0	125	0.983	91	0.999±0.001	7.412±0.003	4.940±0.002	8
0.972	11.7	125	0.972	80	0.999±0.001	7.420±0.005	4.941±0.002	9
0.972	36.0	125	0.976	87	1.002±0.003	7.424±0.008	4.925±0.005	8
0.985	11.7	76	0.975	86	1.002±0.003	7.397±0.010	4.939±0.006	7
0.972	11.7	76	0.964	77	0.998±0.002	7.428±0.005	4.941±0.003	8
0.972	11.7	93	-----	—	0.999±0.003	7.424±0.006	4.939±0.006	6

Table II. Macroscopic density (D_m) of original isotropic and extruded samples and crystallographic data for extrudates. Number of reflections used for unit cell parameters calculations is denoted for each sample. Percent crystallinity of extrudates from DSC data correspond to smoothed values of curves in Fig. 6. Averaged c axis: 2.545±0.001 A°

(*) Precision: ±0.0015 g/cm^3.

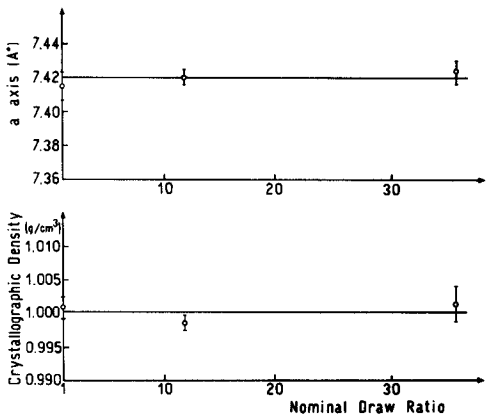

Fig. 3 Crystal data (a axis) and corresponding crystallographic density vs. NDR for FCC extrudates. Extrusion temperature 125°C.

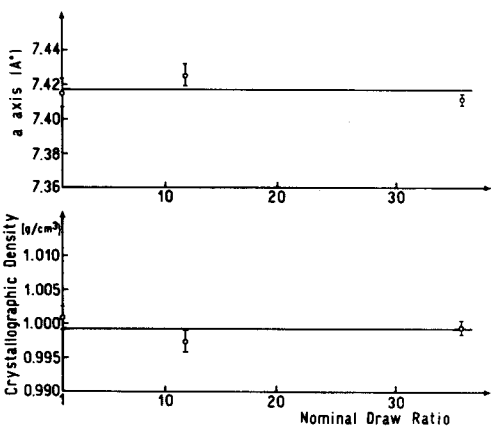

Fig. 4 Crystal data (a axis) and corresponding crystallographic density vs. NDR for ECC extrudates. Extrusion temperature 125°C.

linity = 92, respectively. For ECC extrudates a monotonic decrease in density is observed for both extrusion temperatures; the extent of decrease being more pronounced for the 93°C specimens. FCC extrudates, on the other hand, show the beginning of a minimum at NDR 5.8 which does not proceed further due to the above-mentioned limitations on drawability for low-temperature extrusion. FCC extruded at 125°C not only present a well-defined minimum (Dm = 0.970 g/cm^3) at NDR 4, but also, for NDR 36, reach a value of macroscopic density (Dm = 0.976 g/cm^3) higher than that of the starting, isotropic material (Dm = 0.972 g/cm^3).

It is interesting to note that performing SSE on PE with different initial morphologies provides an opportunity to separate the two opposite density effects discussed in the introduction. Thus, as macroscopic densities of the starting materials increase, Fig. 2, samples with larger lamellar thickness and higher degree of crystallinity become less likely to undergo a density recovery as NDR increases. This correspondence between the amorphous content of the samples and their ability to regain density as a function of NDR, confirms the

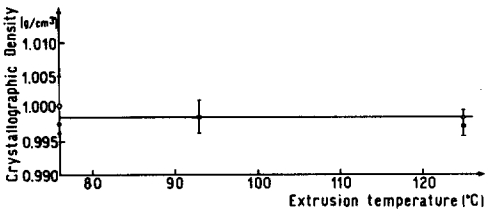

Fig. 5 Crystallographic density vs. extrusion temperature for HDPE of different initial morphologies extruded at NDR 11.7.
◇ Original Dm=0.972 g/cm³
■ Original Dm=0.990 g/cm³
o Original Dm=0.985 g/cm³

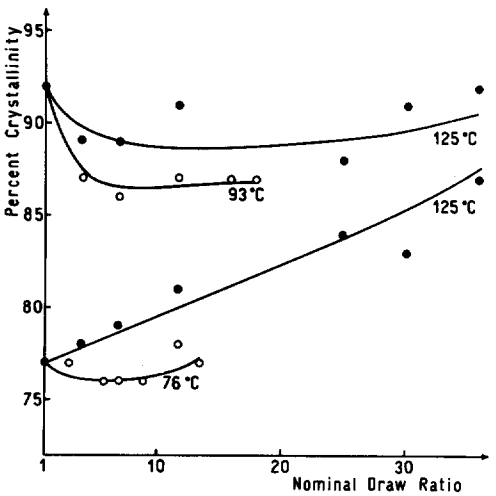

Fig. 6 Percent crystallinity data from DSC vs. NDR for ECC and FCC samples extruded at several different temperatures.

suggestion (9) that the observed macroscopic increase in density follows fundamentally from ordering effects within the amorphous region.

In regard to the mechanism responsible for the density decrease, the data in Table II and the plots in Figs. 3 and 4 show clearly that, within the narrow limits of the experimental error, no variation of unit cell dimensions are observed either for ECC or FCC of PE in the range of NDR from 1 to 36. In addition, Fig. 5 shows the independence of unit cell parameter from extrusion temperature for a series of samples all drawn at the same NDR 11.7. These results clearly rule out the possibility to interpret the density drop upon drawing as an increase in unit cell dimensions, and points to a decrease in the crystalline content during deformation as the only possible mechanism.

Confirmation of these conclusions was derived from differential scanning calorimetry measurements, which, through the heats of fusion, directly lead to the corresponding degrees of crystallinity. The plots in Fig. 6 show the expected density decrease, especially for the case of ECC extruded at 93°C. The apparently anomalous behavior of FCC extruded at 125°C arises surely from the simultaneous annealing process inherent to the DSC method. The eventual occurrence of minima, observed in the cases of morphologies intermmediate between FCC and ECC

(10),depends on the conditions of the experiments and on the total fraction of amorphous material in the original samples.

In conclusion, drawing HDPE by SSE involves: 1.-Increase of the molecular order within the amorphous regions of the material. 2.-Partial transformation of crystalline into amorphous phase. Thus,although drawing of HDPE is an irreversible process,and from the thermodynamic point of view can not be considered to involve fusion,plastic deformation of the specimens proceeds with crystal disorder,accompanied by a decrease in percent crystallinity,and no changes whatsoever in unit cell dimensions.

ACKNOWLEDGEMENTS

INIFTA is a research institute jointly established by the Universidad Nacional de La Plata,the Consejo Nacional de Investigaciones Científicas y Técnicas,and the Comisión de Investigaciones Científicas de la Prov. de Buenos Aires. INTI is the Instituto Nacional de Tecnología Industrial.

The authors wish to thank Prof.R.S.Porter for his endorsement of this project. The donation of equipment by the GTZ (Federal Republic of Germany) through the Partnership Agreement between the Universities of Mainz and La Plata is,as well,gratefully acknowledged.

REFERENCES

1. F.De Candia,R.Russo,V.Vittoria,A.Peterlin,J.Polymer Sci., Polymer Phys.Ed.,20,269 (1982).
2. H.H.Chuah,R.E.De Micheli,R.S.Porter,J.Polymer Sci.,Polymer Letters Ed.,21,791 (1983).
3. W.Glenz,N.Morosoff,A.Peterlin,Polymer Letters,9,211 (1971).
4. A.E.Zachariades,W.T.Mead ,R.S.Porter,Chem.Revs.,80,351 , (1980).
5. H.P.Klug,L.E.Alexander,X-Ray Diffraction Procedures,Chapter 8 p.441, J.Wiley,New York (1970).
6. Fortran Program,BMDPAR,Derivative free non-linear regression Department of Biomathematics,University of California, Los Angeles,C.A. 90024.
7. H.Lipson,H.Steeple,Interpretation of X-Ray Powder Diffraction Patterns,Chapter 6,Macmillan,London.
8. B.Wunderlich,Macromolecular Physics,Vol.2,Chapter 6,p.252, Academic Press,New York (1976).
9. E.W.Fischer,H.Goddar,G.E.Schmidt,J.Polymer Sci.,Part A2 7,37 (1969).
10. R.E.De Micheli,E.M.Macchi,to be published.

Accepted July 9, 1985